



Introduction

While the polar regions comprise only one-eighth of the earth's total surface area, the importance of observations in those regions is becoming increasingly more evident. There are many examples on the influence of the polar regions on lower latitude atmospheric conditions on time scales from synoptic to climatic, space scales from meso to global, and extending through the depth of the troposphere. From a climate perspective, the polar regions are a barometer indicating changes through, for example, glacier extent and permafrost temperature (Hinzman et al. 2005). From a global circulation perspective, Gallimore and Johnson (1981) showed that a meridional Hadley-type circulation extends from the tropics to the poles by thermal forcing on isentropic surfaces. Furthermore, Coherent Tropopause Disturbances (CTDs), which are meso-scale vortices on the dynamic tropopause, have been observed moving from the arctic to near tropical latitudes (Pyle et al. 2004). However, Francis (2002) found that the existing upper-air observation network in high latitudes (Figure 1) is insufficient for the accurate depiction of the tropospheric wind field.

The influence that the polar regions have on lower latitude circulation systems coupled with an inaccurate knowledge of the polar atmospheric state may result in an erroneous picture of global weather systems and subsequent forecasts. One way to improve on that knowledge is to use the proven remote-sensing technique of tracking clouds and other features from weather satellite images. Until recently, this has only been done routinely with geostationary satellites over the middle- and lower-latitudes. Extending this to high-latitudes using polar orbiting satellites presents new challenges. However, Key et al. (2003) showed that the addition of satellite-derived winds over the polar regions has a positive impact on global forecasts.

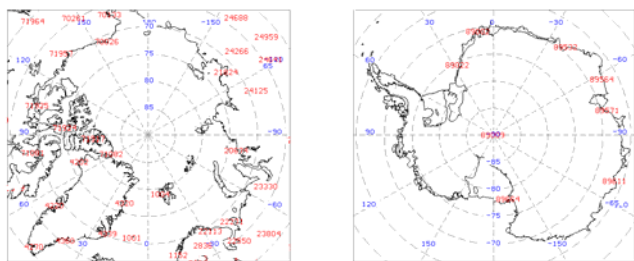


Figure 1: WMO rawinsondes in the polar regions: Arctic (left), Antarctic (right).

Wind Retrieval Methodology

For the past few decades, Atmospheric Motion Vectors (AMV) have been primarily derived from a time-sequence of images from geostationary satellites. More recently, this algorithm has been applied to data from polar orbiting satellites and these AMVs are now routinely input into many operational global models. The technique is based on the geostationary satellite winds algorithm, using MODIS data from the polar orbiting Terra and Aqua satellites. Three successive passes over the poles (Figure 2) are used.

Targeting

- Clouds in the IR window channel 11 μm
- Water vapor features in 6.7 μm

Tracking

- Cross-correlation technique
- GFS 6, 9, and 12-hour forecast grids as first guess
- Image triplets (rather than pairs) are used for consistency check

Wind height assignment

IR window or H₂O-ice using the temperature profile forecasts from GFS.

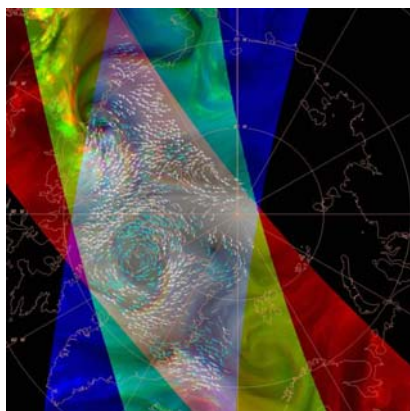


Figure 2: Three overlapping Aqua MODIS passes, with WV and IR winds superimposed. The white wind bars are above 400 hPa, cyan are 400 to 700 hPa, and yellow are below 700 hPa. Each pass is shown in a different color: red, green, and blue. The intersection is the gray region, where the winds are derived.

Mechanisms that Propagate Wind Information to Lower Latitudes

Using a pre-operational version of the National Centers for Environmental Prediction's (NCEP) Global Forecast System (GFS), a side-by-side experiment was run for a six week period during the late summer of 2004, with and without the MODIS polar winds.

The addition of the MODIS winds resulted in an improved or neutral impact in the 120-hour forecast for 70% of the days for the 500 hPa heights over the northern hemisphere. The MODIS winds are only derived poleward of 65° latitude. What are possible explanations for this global impact? **Five forecast cases were examined to determine how winds in the Arctic affect the wind and geopotential height fields in the jet stream region, resulting in changes in wave propagation speed evident in later forecasts.**

A relationship was derived that equates the divergence of the ageostrophic wind to vorticity advection:

$$\nabla \cdot \vec{V}_a = -\frac{1}{f_0} \vec{V}_g \cdot \nabla \zeta_g$$

Since vorticity advection is an indicator of the propagation speed of troughs and ridges, differences in the ageostrophic wind will, therefore, be a similar indicator.

Figure 3 is a field of differences of the divergence of ageostrophic wind from the model runs with and without the MODIS winds. The ovals indicate the largest differences, which are coincident with the jet stream. Figure 4 depicts the differences in the 1000-500 hPa thickness fields between the two model runs. On the left is the initialization time; on the right is the 72-hour forecast. The position of the red and blue features on the right side indicate the this trough/ridge system was slowed in the MODIS winds model run, as compared to the control; which is in the vicinity of the largest differences in the advected divergence of the ageostrophic wind.

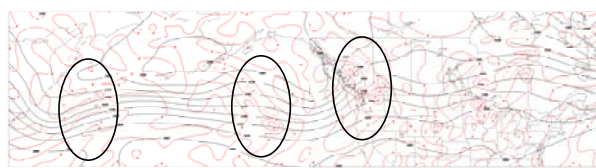


Figure 3: Difference in the divergence of the ageostrophic wind (10^{-5} s^{-1}) at 500 hPa between the MODIS winds and control model runs over the North Pacific Ocean. This is equivalent to the difference in vorticity advection. The largest differences are circled. This is the analysis at 0000 GMT on 11 September 2004.

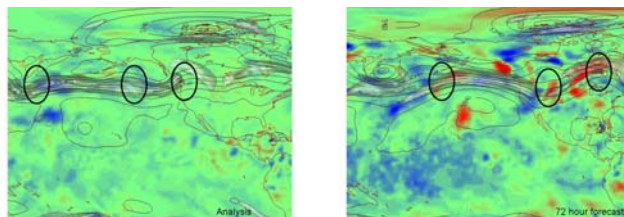


Figure 4: The analysis (left) and 72-hour forecast (right) showing differences in the 1000-500 hPa thickness, along with the MODIS 500 hPa heights. The ovals are from Figure 3. Positions of ovals in the 72-hour forecast represent a subjective positioning using intermediate forecast times to guide. The color range from blue to red denotes a range of -30 to +30 gpm difference. Near zero difference is in green. The 30 m s⁻¹ wind speed, representing the jet stream, is in transparent white.

Forecast Impact: Tropical Cyclone Position

Hurricane Karl, which remained in the mid-Atlantic Ocean throughout its lifetime, moved generally northwestward for several days "until 22 September when it turned northeastward in response to a deep-layer baroclinic trough developing north of the hurricane." (Beven 2004) The model containing the MODIS winds held back the advancement of this trough which permitted the forecast position of Karl to track farther west than the control (Figure 5). This resulted in an improved forecast track for Hurricane Karl in the 96-hour forecast, although it was still too far east (MODIS: 19.3°N 45.4°W; Control: 18.7°N 43.0°W) instead of 18.7°N 47.0°W. This is an error of 184 km and 424 km, respectively.

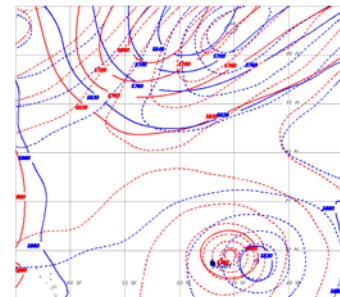


Figure 5: Hurricane Karl over the Atlantic Ocean in the 96-hour forecast from 0000 GMT 17 September 2004. Solid red contours are the 500 hPa heights with MODIS winds; dashed red are 1000 hPa heights. Solid blue are 500 hPa heights of the control; dashed blue are 1000 hPa heights. Actual position at the forecast time of hurricane Karl is shown with the hurricane symbol.

Conclusions

From the five cases examined, it was determined that the addition of the polar winds modifies the mass balance in synoptic-scale waves near the polar jet streams, more consistently in data void regions. This change in mass balance is evident in differences in the ageostrophic wind, which has an effect on the speed and amplitude of baroclinic waves that extends from the jet stream into lower latitudes in later forecast times. These results reveal the substantial impact that polar-only observations have on the predictability of global weather systems.

Acknowledgments: The research was supported, in part, by NOAA grant NA07EC0676 and NASA grant NASS31367.
Contact: Dave Santek dave.santek@ssec.wisc.edu

Beven, J., 2004. Tropical Cyclone Report: Hurricane Karl. Retrieved 27 April 2007 from <http://www.nhc.noaa.gov/2004karl.shtml>.
Francis, J. A., 2002. Validation of reanalysis upper-level winds in the Arctic with independent rawinsonde data. *Geophys. Res. Lett.*, 29, No. 9.
Gallimore, R. and D. Johnson, 1981. The forcing of the meridional circulation of the isentropic zonally averaged circumpolar vortex. *J. Atmos. Sci.*, 38, 583-599.
Hinzman L.D., et al., 2005. Evidence and implications of recent climate change in northern Alaska and other Arctic regions. *Climatic Change*, 72, 251-298.
Key, J. R., D. Santek, C. S. Velden, N. Bornmann, J.-N. Thépaut, L. P. Risholmgard, Y. Zhu, and W. P. Menzel, 2003. Cloud-Drift and Water Vapor Winds in the Polar Regions from MODIS. *IEEE Trans. Geosci. Remote Sens.*, 41, 482-492.
Pyle, M., D. Keyser, L. Bosart, 2004. A diagnostic study of jet streaks: kinematic signatures and relationship to coherent tropopause disturbances. *Mon. Wea. Rev.*, 132, 297-319.